JOURNAL OF MATERIALS SCIENCE 32 (1997) 755–760

Fatigue life prediction of composites under two-stage loading

NOBUO OTANI
Maebashi City College of Technology, 460 Kamisadori-cho, Maebashi-City 371, Japan
DONG-YEUL SONG
Research Center for Advanced Science and Technology, University of Tokyo, 4-6-1 Komaba, Meguro-ku, Tokyo 153, Japan

In order to predict the fatigue life under two-stage loading by formulating a cumulative fatigue damage rule for composite materials, the fatigue process in SiC–Al and glass-fibre reinforced plastics were investigated. A microcrack occurred within the composites which resulted in cumulative fatigue damage that increased linearly with the number of cycles. The mechanical conditions of damage growth and failure were determined by characterizing the microdamage governing the fatigue. The ultimate failure is shown to occur when the product of the stress amplitude ratio and microdamage density is beyond a critical value and an expression for the remaining fatigue life is derived.

1. Introduction

Metal matrix composites (MMCs) and polymer matrix composites (PMCs) are extensively available as engineering materials for structural applications. In the engineering analysis and design of composite structures, reliability under service conditions is a major concern. This involves studying the cyclic fatigue degradation and the failure of the composite under repeated loading. It is therefore, important to establish an evaluation approach for the reliability of multiple fatigue loading. Reliability theory applied to multiple fatigue loading is known to be related to cumulative damage theory, which has been extensively studied. Miner [1] assumed that cumulative fatigue damage was proportional to the total work absorbed by a specimen and found that failure occurred if Equation 1 was satisfied.

$$\sum_{i=1}^{n} \frac{n_i}{N_i} = 1 \tag{1}$$

where n_i represents the number of cycles applied at a given stress level σ_i and N_i is the number of cycles to failure at this stress level. Broutman and Sahu [2] reported that the reduction of the residual strength of a composite depended on the extent of the cumulative fatigue damage and that the stress amplitude decreased linearly. They also showed that the cumulative fatigue life for two-stage loading, based on the assumption that the strength reduction at a given stress level was not affected by precycling at a different stress level, could be represented as

$$\frac{(1 - S_1)}{(1 - S_2)}\left(\frac{n_1}{N_1}\right) + \left(\frac{n_2}{N_2}\right) = 1 \tag{2}$$

where $S_1 = \sigma_1/\sigma_B$, $S_2 = \sigma_2/\sigma_B$; σ_1 and σ_2 are the cyclic stress of the first and second stage, respectively and σ_B is the tensile strength. Hashin and Rotem [3] assumed that various damages represented by the S–N curve added logarithmically and proposed the following expression

$$\left(\frac{n_1}{N_1}\right)^{\frac{1 - S_2}{1 - S_1}} + \left(\frac{n_2}{N_2}\right) = 1 \tag{3}$$

Manson and Halford [4] regarded the crack length as an indicator of fatigue damage and developed Equation 4 by introducing the extent of the normalized crack length as the damage level.

$$\left(\frac{n_1}{N_1}\right)^{\left(\frac{n_1}{N_2}\right)^{0.4}} + \left(\frac{n_2}{N_2}\right) = 1 \tag{4}$$

As previously mentioned, only a few theories based on the actual fatigue damage behaviour exist, notably that of Manson and Halford [4]. Thus, it is difficult to precisely evaluate the reliability of a structure even if the damage is identified in service. At this point, the Manson and Halford theory can evaluate the extent of fatigue damage by reference to the surface crack length. However, the application of this theory to composite materials, where internal damage plays an important role in fatigue, is inappropriate [5–7].

The purpose of this study is to predict the remaining fatigue life by establishing a cumulative fatigue damage rule for composite materials. To this end, the fatigue process of SiC–Al and glass fibre reinforced plastic (GFRP) is investigated and the microdamage

0022–2461

governing the fatigue is characterized. In addition, we determine the conditions for damage growth and failure, that are closely related to consideration of a cumulative fatigue damage rule and prediction of the fatigue life.

2. Experimental procedure

2.1. Tested materials

Two different composites, firstly a silicon carbide whisker reinforced aluminium alloy (SiC–Al; fibre volume fraction, $V_f = 20$ vol.% and glass fibre reinforced plastic (GFRP; fibre volume fraction, $V_f = 45$ vol.%), were prepared. The SiC–Al composite was sintered using powder metallurgy techniques and then extruded as a cylindrical rod 10 mm in diameter. This was cut into the specimen as shown in Fig. 1. The GFRP contained 10 plies of the laminate reinforced with 8 satin woven glass fabrics (2.7 mm in thickness). The resin matrix was polyester. The specimen was 20 mm in width and 250 mm in length (Fig. 1). The mechanical properties of these materials were: SiC–Al; $\sigma_B = 680$ MPa, $E = 108$ MPa. GFRP; $\sigma_B = 309$ MPa, $E = 21.2$ MPa where E is the Young's modulus.

2.2. Low cycle fatigue tests

The fatigue tests were conducted in a servohydraulic testing machine. The specimens were mounted with chuck distances of 100 mm (GFRP) and 50 mm (SiC–Al). The fatigue tests were performed at room temperature with a sine waveform at a frequency of 5 Hz. The minimum to maximum stress ratio R was kept at zero throughout the tests. The stress amplitude ratio S $(=\sigma_{1,2}/\sigma_B)$, based on the tensile strength σ_B obtained from the static tension test, was between 0.4–0.9. The S–N curve was determined by measuring the number of cycles N to failure at each constant stress amplitude as is shown in Fig. 2 (each point on the S–N curve represents the average value of 6 data points).

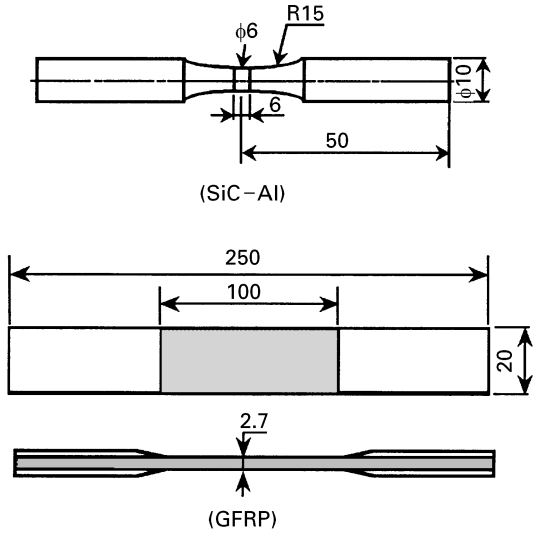

Figure 1 Specimen configurations (unit: mm).

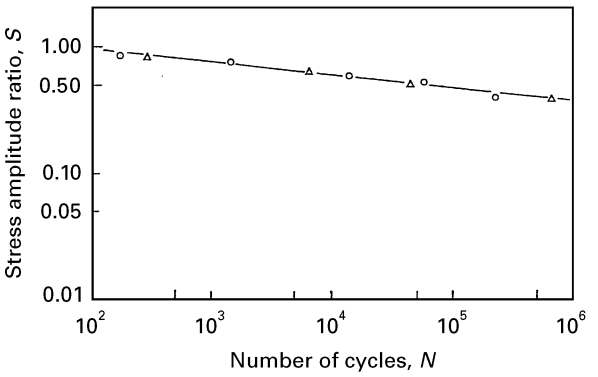

Figure 2 S–N curve at each constant stress amplitude in (○) SiC–Al and (△) GFRP.

2.3. Microscopic damage measurement

Microscopic damage on the side and vertical section of specimens during fatigue loading were observed and measured by using an optical microscope. These damages were quantitatively represented as follows:

$$\rho = \rho_t = \frac{\dfrac{\sum a}{A_0}}{\dfrac{\left(\sum a\right)_{N=10^6}}{A_0}} \tag{5}$$

where ρ_t is the normalized transverse crack density in a 90° layer of GFRP, ρ is the normalized internal microcrack density of SiC–Al, a is the microcrack length and A_0 is the observed area. Also, $N = 10^6$ represents the number of cycles at failure.

2.4. Two-stage loading fatigue tests

In the low cycle region, two-stage loading fatigue tests were conducted, i.e., Hi–Lo (first stage fatigue; high stress amplitude σ_1, the number of cycles n_1, and second stage fatigue; low stress amplitude σ_2, the number of cycles n_2) and Lo–Hi (first stage fatigue; low stress amplitude σ_1, the number of cycles n_1, and second stage fatigue; high stress amplitude σ_2, the number of cycles n_2).

3. Results and discussion

3.1. Prediction of remaining fatigue life

Fig. 3 shows the remaining life values obtained from the two-stage loading fatigue tests on SiC–Al (high stress amplitude; $S = 0.79$, low stress amplitude; $S = 0.50$) and also indicates the results predicted by the various cumulative fatigue damage theories. It can be seen from this figure that the difference between the prediction using the model of Miner [1] and the experimental results is very large. In particular, the prediction for Lo–Hi fatigue loading is very poor. This trend is also observed for the application of the model of Hashin and Rotem [3].

The theory of Manson and Halford [4] which is a prediction based on microdamage, predicts opposite behaviour than observed in these experiments for both

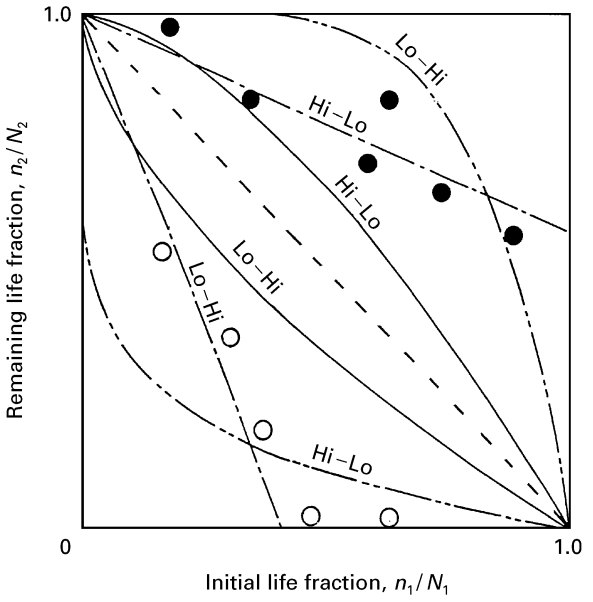

Figure 3 Comparison of the (●) Hi-Lo and (○) Lo-Hi experimental results and predicted values for the remaining fatigue life under two-stage loading in SiC–Al. Using the models of; (. . . .) Miner, [1], (——) Hashin and Rotem [3], (–·–) Broutman and Sahu [2] and (—· ·—) Manson and Halford [4].

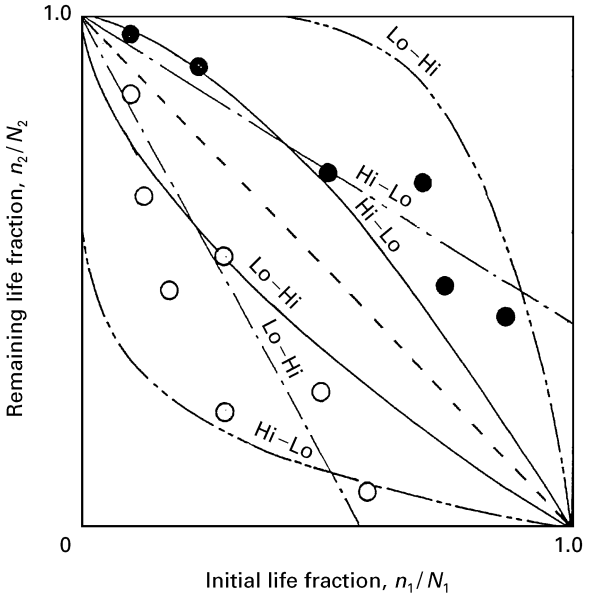

Figure 4 Comparison of the (●) Hi-Lo and (○) Lo-Hi experimental results and predicted values for the remaining fatigue life under two-stage loading in GFRP using the models of; (. . . .) Miner, [1], (——) Hashin and Rotem [3], (–·–) Broutman and Sahu [2] and (—· ·—) Manson and Halford [4].

Hi–Lo and Lo–Hi fatigue loading. On the other hand, the observed agreement between the values obtained using the model of Broutman and Sahu [2] and the experimental results is very good for both the Lo–Hi and Hi–Lo fatigue loading cases.

Fig. 4 shows the values for the remaining life obtained from the two-stage loading fatigue tests on GFRP (high stress amplitude; $S = 0.70$, low stress amplitude; $S = 0.48$). It can be seen from this figure that the nonlinear behaviour for the remaining fatigue life is somewhat less as compared with the case of SiC–Al. However, the trend for both Lo–Hi and Hi–Lo fatigue loading are identical to the SiC–Al case. That is, the case of the Lo–Hi loading indicates shorter remaining life compared with Miner's rule but the case of the Hi–Lo loading shows longer remaining life as compared with Miner's rule. In addition, predictions using the Manson and Halford model are the same as those for the case of the SiC–Al.

With regard to the results obtained using the model of Broutman and Sahu [2] it should be noted that the case of the Lo–Hi loading indicates somewhat short remaining life as compared with the model which is slightly deviated from the experimental results for the Hi–Lo loading. On the other hand, the theory of Broutman and Sahu is based on the assumption that the remaining strength linearly decreases with the number of cycles. Unfortunately, it has been reported that the actual remaining strength decreases in a nonlinear manner with the number of cycles [8–10].

From the above results, it can be recognized that a cumulative fatigue damage theory that describes the actual damage and mechanical behaviour and could be applied to the case of both the SiC–Al and GFRP composites has not yet been developed. Therefore, in order to obtain a general cumulative fatigue damage rule based on actual fatigue damage, the microscopic fatigue damage processes of these two composites have been investigated. These results will be discussed in the following sections.

3.2. Microscopic observation of fatigue process

3.2.1. Fatigue process of SiC–Al composites

We will initially discuss results on surface crack development in SiC–Al composites. Figs 5 and 6 show the relationship between the surface crack length a_s and the ratio of the number of cycles n/N at $S = 0.50$ and $S = 0.79$, respectively. In the case of the stress amplitude ratio of 0.5, the surface crack grows by nearly 0.26 mm in length during the initial fatigue and then no further growth takes place. However, for the stress amplitude ratio of 0.79, the surface crack is

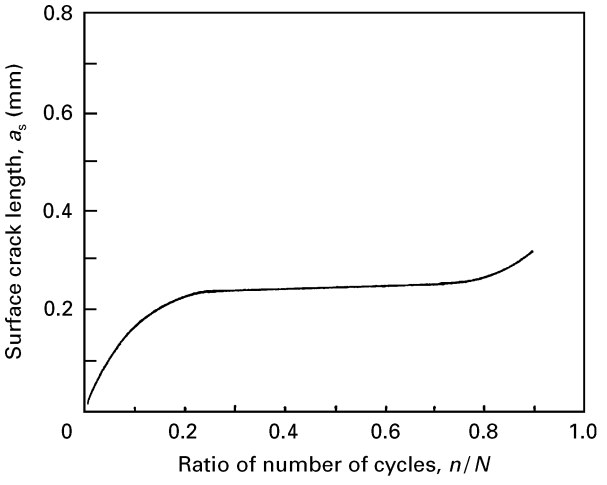

Figure 5 Relationship between surface crack length and ratio of number of cycles at a stress amplitude ratio of $S = 0.5$ in SiC–Al. (Here, a_s indicates the maximum surface crack length at each n/N.)

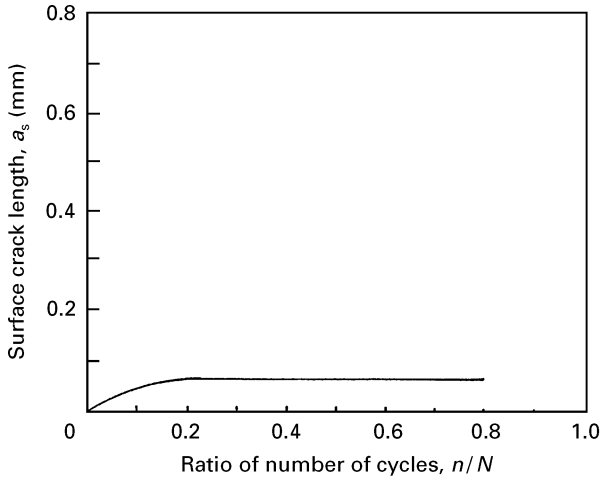

Figure 6 Relationship between surface crack length and ratio of number of cycles at a stress amplitude ratio of $S = 0.79$ in GFRP. (Here, a_s indicates the maximum surface crack length at each n/N.)

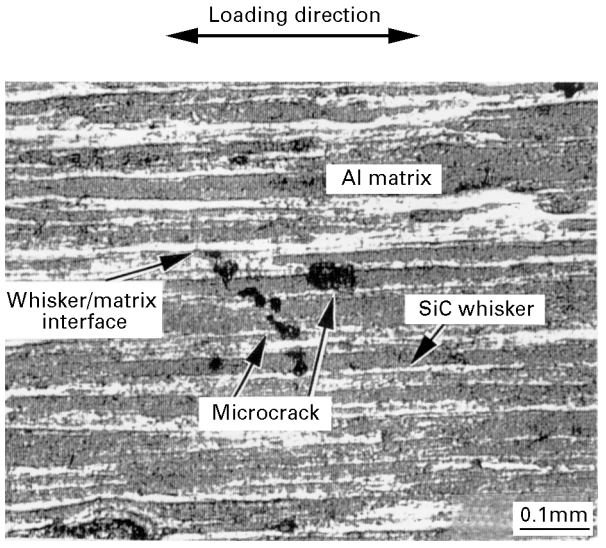

Figure 7 Photomicrography of internal microcracks occurred in SiC whisker layer.

much smaller than that in the case of $S = 0.50$. Also, the maximum surface crack length is only 0.07 mm and macroscopic crack growth hardly occurred.

In addition, from observation of this surface crack growth in the thickness direction of the specimen, it was found that no further crack growth happened since the crack was almost arrested by a SiC whisker layer. Therefore, it can be concluded that surface cracks do not play an important role in SiC–Al fatigue as compared with the case of metal fatigue. Fig. 7 shows the internal microcrack that occurred in the SiC whisker layer at the initial fatigue loading. This microcrack was also observed at the whisker/matrix interfaces and it increased with the number of cycles. Fig. 8 shows the variation of the normalized microcrack density ρ with the number of cycles n.

Thus, we can predict that final failure occurs due to the coalescence of these internal microcracks and that the fatigue of SiC–Al proceeds via the growth of the internal microcrack.

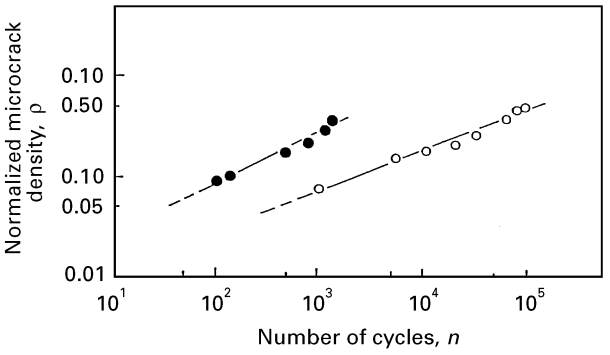

Figure 8 Relationship between normalized microcrack density and number of cycles in SiC–Al. Data is shown for s values of (●) 0.79 and (○) 0.50.

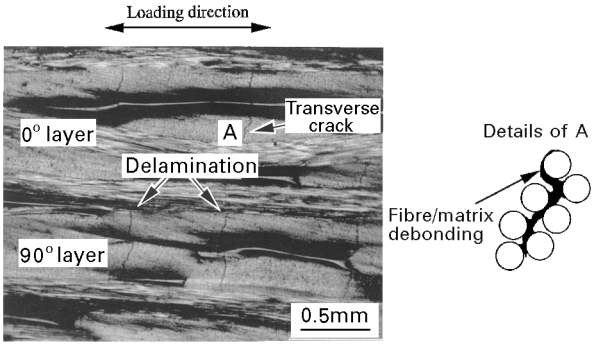

Figure 9 Photomicrography of the microdamage that occurred in a transverse fibre bundle (90° layer) in satin woven glass fibre polyester composites (GFRP).

3.2.2. Fatigue process of GFRP composites

At the beginning of the cycles, debonding occurred at the fibre/matrix interfaces in a transverse fibre bundle (90° layer) as is shown in Fig. 9. This debonding increased with an increase in the number of cycles and became a transverse crack. As the number of cycles increased, this transverse crack reached a 0° layer and produced delamination at the interface. After that, the delamination propagated along the interface. Thus, ultimate failure of the composites occurred due to the coalescence of the transverse crack and delamination. Fig. 10 shows the relationship between the normalized transverse crack density $\rho_t = \rho$ and the number of cycles n for both stress amplitude ratios ($S = 0.48$ and $S = 0.70$).

From the above results, it can be seen that the fatigue damage of GFRP contained contributions from a transverse crack, delamination and fibre breakage in the longitudinal direction. However, from the point that the initiation and growth of the delamination resulted from a transverse crack, it can be approximately considered that the GFRP fatigue is effectively governed by the transverse crack.

3.4. The relationship between microscopic damage and remaining fatigue life

As previously mentioned, it has been identified that the fatigue process of SiC–Al and GFRP are governed by internal microcracking and transverse cracking, respectively. In addition, the normalized crack density

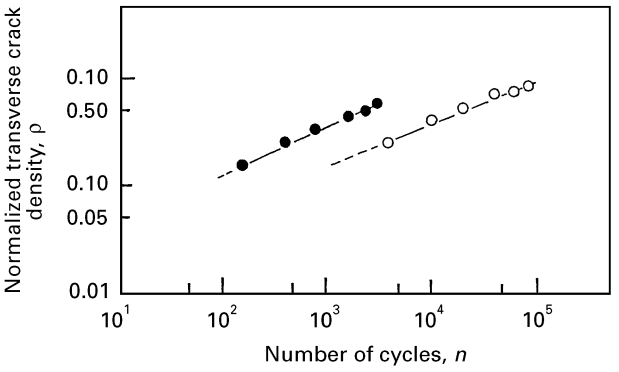

Figure 10 Relationship between normalized transverse crack density and number of cycles in GFRP. Data taken for s values of; (●) 0.70 and (○) 0.48.

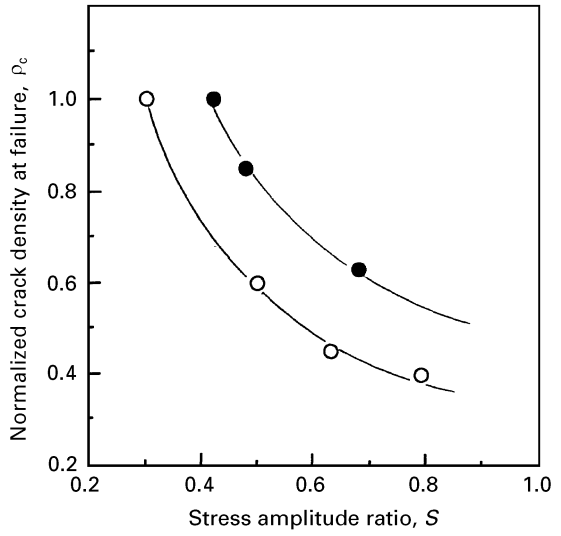

Figure 11 Relationship between stress amplitude ratio and normalized crack density at failure in (○) SiC–Al and (●) GFRP.

ρ was found to linearly increase in proportion to the number of cycles n for both the SiC–Al and GFRP cases. This trend was identical in the case of each stress amplitude.

Thus, these relationships can be expressed in a simple form as

$$\rho_i = kS_i^a * n_i^b \tag{6}$$

where k, a and b are constants. The values of a and b obtained from Figs 8 and 10 are as follows:

$$\text{SiC–Al; } a = 4.0,\ b = 0.5$$

$$\text{GFRP; } a = 4.0,\ b = 0.48$$

On the other hand, Fig. 11 shows the relationship between the stress amplitude ratio S and the normalized crack density at failure ρ_c, where the normalized crack density of SiC–Al and GFRP correspond to the normalized internal microcrack density and normalized transverse crack density, respectively. It is seen from this figure that the failure in both SiC–Al and GFRP cases occurs when the following expression is satisfied.

$$S_i^x * \rho_{ic}^y = Const. \tag{7}$$

where the values of x and y obtained from this figure are equal to 1 for both SiC–Al and GFRP. While, the S–N curve, as shown in Fig. 2, can be approximately expressed as follows:

$$S_i^z * N_i = Const. \tag{8}$$

where z is a constant. Thus, from Equations 6 and 8, it can be considered that the fatigue process is explained by the following expression

$$S_i^{\frac{a}{b}} * n_i = \left(\frac{\rho_i}{k}\right)^{\frac{1}{b}} \tag{9}$$

Moreover, at the point where the specimen failed, n_i and ρ_i become N_i and ρ_{ic}, respectively. So, Equation 9 becomes

$$S_i^{\frac{a}{b}} * N_i = \left(\frac{\rho_{ic}}{k}\right)^{\frac{1}{b}} \tag{10}$$

Thus, the failure for the multiple stage (m-stage) fatigue occurs when Equation 11, obtained from Equations 9 and 10 is satisfied

$$\sum_{i=1}^{m} S_i^{\frac{a}{b}} n_i = \left(\frac{\rho_{mc}}{k}\right)^{\frac{1}{b}} \tag{11}$$

Also, substituting Equations 7 and 10 which represent the failure condition into Equation 11, a general expression for the multiple stage fatigue is obtained as follows:

$$\sum_{i=1}^{m} \left(\frac{S_m}{S_i}\right)^{\frac{1}{b}} \left(\frac{n_i}{N_i}\right) = 1 \tag{12}$$

Thus, substituting $m = 2$ and $b = 0.5$ for both SiC–Al and GFRP into Equation 12, the remaining life for two-stage fatigue loading in SiC–Al and GFRP composites is given by

$$\left(\frac{S_2}{S_1}\right)^2 \left(\frac{n_1}{N_1}\right) + \left(\frac{n_2}{N_2}\right) = 1 \tag{13}$$

Fig. 12 shows a comparison between the experimental results and predictions using Equation 13 and the

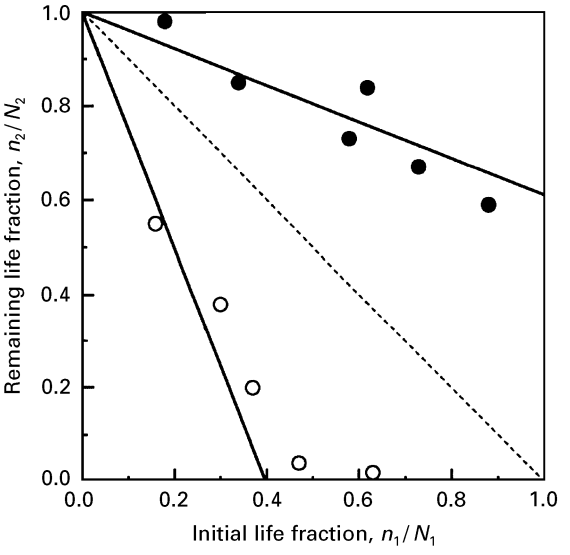

Figure 12 Comparison of (●) Hi-Lo and (○) Lo-Hi experimental results and theoretical prediction for remaining fatigue life under two-stage loading in SiC–Al using the model of (. . . .) Miner [1]. The fit to the Hi-Lo data is using Equation 13 and the fit to the Lo-Hi data is also using Equation 13.

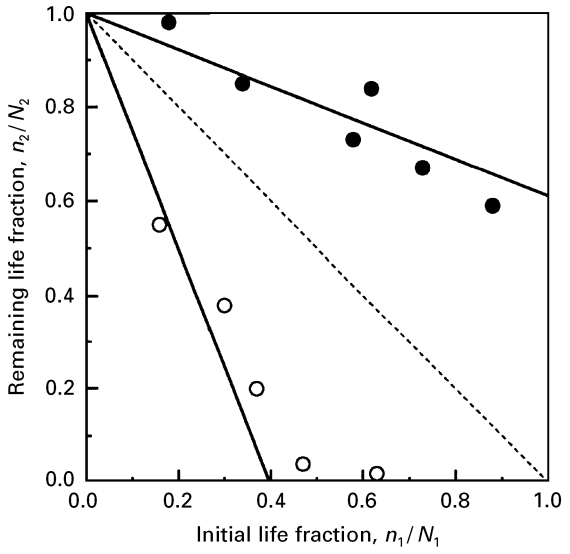

Figure 13 Comparison of (●) Hi-Lo and (○) Lo-Hi experimental results and theoretical prediction for remaining fatigue life under two-stage loading in GFRP using (– – –) the model of Miner [1]. The fit to the Hi-Lo data is using Equation 13 and the fit to the Lo-Hi data is also using Equation 13.

Miner rule for two-stage fatigue loading in SiC–Al (where, experimental values represent the average of 6 data points). For both Hi–Lo and Lo–Hi loading, the theoretical prediction of Equation 13 closely agrees with the experimental results. Fig. 13 represents the results for GFRP (where, experimental values represent the average of 6 data points). It is suggested from this figure that the prediction using Equation 13 indicates a little short remaining life compared with the experimental results for both Lo–Hi and Hi–Lo loading but this difference is small compared with the prediction of Broutman and Sahu [2].

Therefore, it can be concluded that the remaining life for two-stage fatigue loading in SiC–Al and GFRP composites can be approximately predicted using Equation 13.

4. Conclusions

In order to predict the fatigue life under two-stage fatigue loading by establishing a cumulative fatigue damage rule for SiC–Al and GFRP composites, the fatigue process was investigated and characterized in terms of micro damage governing the fatigue. Moreover, the conditions of damage growth and failure were determined and were shown to be closely related to the consideration of a cumulative fatigue damage rule and the prediction of the fatigue life. The results obtained are as follows:

(1) The fatigue process of composite materials is governed by the internal crack density. Normalized crack density can be represented as follows:

$$\rho_i = kS_i^a n_i^b$$

where S_i is the ratio of stress amplitude, n_i is the number of cycles and k, a and b are constants.

(2) The failure condition can be expressed by using the constants x and y as follows:

$$S_i^x \rho_{ic}^y = Const.$$

(3) The remaining life for two-stage fatigue loading can be predicted from the following expression

$$\left(\frac{S_2}{S_1}\right)^2 \left(\frac{n_1}{N_1}\right) + \left(\frac{n_2}{N_2}\right) = 1$$

References

1. M. A. MINER, *J. Appl. Mech.* **12** (1945) A159.
2. L. J. BROUTMAN and S. SAHU, in Composite Materials: Testing and Design ASTM STP 497 (American Society for Testing and Materials, Philadelphia, PA, 1972) p170.
3. Z. HASHIN and A. ROTEM, *Mater. Sci. Engng* **34** (1978) 147.
4. S. S. MANSON and G. R. HALFORD, *Int. J. Frac.* **17** (1981) 169.
5. A. KOBAYASHI and N. OTANI, in Proceedings of the 13th Symposium of the International Committee on Aeronautical Fatigue, Pisa, Italy, May 1985, edited by A. Salvetti and G. Cavallini (EMAS, 1985) p. 247.
6. K. L. REIFSNIDER and A. L. HIGHSMITH, "Materials: Experimentation and Design in Fatigue" (Westbery House, Guildford, Surrey, 1981) p. 246.
7. B. HARRIS, *AGARD Lect. Ser.* **118** (1981) 6.1.
8. L. J. BROUTMAN and S. SAHU, in Proceedings of the 24th Annual Technical Conference, Washington D.C. 1969, Reinforced Plastics/Composites Division (Society of Plastics Industry Inc., 1969) p. 11-D.1.
9. A. KOBAYASHI and N. OTANI, in Proceedings of the 14th Symposium of the International Committee on Aeronautical Fatigue, Ottawa, Canada, June 1987, edited by D. L. Simpson (EMAS, 1987) p. 195.
10. J. T. FONG, Damage in Composite Materials ASTM STP 775, edited by K. L. Reifsnider (American Society for Testing and Materials, Philadelphia, PA, 1982) p 243.

Received 7 June 1995
and accepted 13 June 1996